Available online at www.sciencedirect.com
ScienceDirect
Precision Engineering 32 (2008) 196–206
PRECISION ENGINEERING
www.elsevier.com/locate/precision

Evaluation of surface roughness based on monochromatic speckle correlation using image processing

B. Dhanasekar [a], N. Krishna Mohan [b], Basanta Bhaduri [b], B. Ramamoorthy [a,*]

[a] *Manufacturing Engineering Section, Department of Mechanical Engineering, Indian Institute of Technology Madras, Chennai 600036, India*
[b] *Applied Optics Laboratory, Department of Physics, Indian Institute of Technology Madras, Chennai 600036, India*

Received 19 April 2007; received in revised form 14 August 2007; accepted 21 August 2007
Available online 28 August 2007

Abstract

The measurement of roughness on machined surfaces is of great importance for manufacturing industries as the roughness of a surface has a considerable influence on its quality and function of products. In this paper, an experimental approach for surface roughness measurement based on the coherent speckle scattering pattern caused by a laser beam on the machined surfaces (grinding and milling) is presented. Speckle is the random pattern of bright and dark regions that is observed when a surface is illuminated with a highly or partially coherent light beam. When the illuminating beam is reflected from a surface, the optical path difference between various wavelets with different wavelength would result in interference showing up as a granular pattern of intensity termed as speckle. The properties of this speckle pattern are used for estimation/quantification of roughness parameters. For measurement of surface roughness, initially the speckle patterns formed are filtered in the spatial frequency domain. The optical technique, namely spectral speckle correlation (autocorrelation) is utilized in this work for the measurement of roughness on machined surfaces. It has been observed that the pattern formed is dependent on the roughness of the illuminated surface. For example, a rough surface (milled) shows a small central bright region with a rapid decrease in intensity towards the edges, while a smooth surface (ground) shows a large central bright region with gradually decreasing intensity towards the edges. The complete methodology and analysis for quantification/estimation of surface finish of milled and ground surfaces based on speckle images that could be implemented in practice, is presented in this paper.

Keywords: Speckle image; Speckle correlation; Autocorrelation; Surface roughness

1. Introduction

The quality assessment of engineering surfaces with respect to their functional and optical properties for various loading conditions is influenced by roughness parameters, which characterize basically the surface micro topography. In many industrial applications such as production and processing of metals, semiconductors (wafers), ceramics, paper and plastic—roughness measurement is an essential part of the quality inspection. Despite the importance of the surface microtopography, the task of an in-situ or even in-process measurement has not been solved adequately, as yet. Until today, these measurements are usually performed using linearly probing instruments, such as mechanical and optical profilometers [1,2]. The results are well-specified roughness parameters, e.g. the rms-roughness R_q or the arithmetic mean of the surface heights R_a (ISO 4287), which are calculated from the sampled surface profile. The conventional method for measuring surface roughness is to pass a stylus probe across the surface and monitor its movement such that the surface microprofile can be traced. These devices are very sensitive, and the diamond stylus could scratch the surface particularly when the materials are soft. A common drawback of this approach is the small area using which the roughness is evaluated at any one time and also the transducer is very sensitive and the stylus tip is fragile. Therefore, the instrument must be handled carefully in a fairly, clean environment. Another problem with the stylus measurement technique is the size of the stylus radius and the crevices of the surface. If the crevices are narrow such that the stylus cannot penetrate all the way to the bottom, the measurement will not be accurate and cannot be a true representation of the surface. These drawbacks [3–5] explain the need and the importance for non-contact techniques for measurement of surface roughness. With the development of lasers, modern optics, and photodiode arrays, the technique of applying

* Corresponding author. Fax: +91 44 22575705.
E-mail address: ramoo@iitm.ac.in (B. Ramamoorthy).

0141-6359/$ – see front matter © 2007 Elsevier Inc. All rights reserved.
doi:10.1016/j.precisioneng.2007.08.005

light scattering for surface roughness has received a considerable attention.

On projecting a coherent light to a rough surface, the reflected waves from different points of the surface interfere and form speckles. Fully developed speckles are due to the destructive interference as the phase difference between waves is equal to half of the wavelength of the light source used (λ/2). A surface having roughness of λ/4 gives a path difference of λ/2 for normal incidence. From a fully developed speckle pattern, the contrast of the same can be used as a roughness parameter. Persson [6] described a speckle-contrast technique for real-time measurements of surface roughness. The experimental used in that work had only a laser and a video camera for recording. The technique was verified with measurements of roughness in the range of R_a (using stylus instrument) was from 0.010 to 0.150 μm. Persson [7] also presented measurements of roughness on rough machined surfaces using the spectral speckle correlation technique. Two light sources of different wavelengths were used and an appropriate choice of wavelength difference, the sensitivity of measurement is optimized. The reported measuring range of R_a was from 0.5 to 5 μm, which is a much-improved result from that of the speckle-contrast technique. However, this technique was reported to be very sensitive to misalignment and vibrations. Further, for use under dynamic conditions, the two speckle patterns have to be obtained from the exact spot of the specimen surface and measured simultaneously, which is difficult to implement. A theoretical study concerning applications of speckle-correlation methods to surface-roughness measurement was reported by Ruffing [8]. Tay et al. [9] have described optical techniques for surface-roughness measurements that are generally based on the light-scattering. In this method, the roughness-height information of surfaces is obtained from the average intensity scattered in the specular direction, while the autocorrelation function of surface height is determined from the average intensity scattered away from the specular direction. These investigations, which are based on Beckmann's [10] rough-surface scattering theory, are applicable only to surfaces within a moderately rough range, usually not more than 4 μm of R_a value. Another optical method for roughness measurements is the speckle pattern contrast method [11], which involves illuminating the test surface normally with a collimated laser beam. From the average contrast of the resulting far-field speckle (or an image speckle) pattern, the surface roughness can be obtained. Sprague and Thompson [12] have first proposed a technique for measurement of the surface-roughness properties utilizing the contrast of speckle patterns. Later, Yoshimura et al. [13] have extensively studied the statistical properties of speckle intensity variations produced at the image and diffraction planes for estimation of surface roughness. On the basis of these studies, a method using the contrast of speckle patterns for non-contact measurements of the surface roughness has been applied to various actual objects. Yamaguchi et al. [14] have analysed the solid surfaces by speckle correlation of video signals to measure the roughness. In their study, speckle patterns appearing in the diffraction field of a laser-illuminated sample are captured using a CCD camera before and after the change of the incident angle or the laser wavelength, and then based on their cross-correlation surface roughness was evaluated. Lukaszewsk et al. [15] showed that certain features of the speckles observed in the angular distribution for the intensity of light reflected from rough surfaces can be used for the on-line quality control of components produced by casting process.

In this paper, the speckle patterns of the machined surfaces (ground and milled) are first captured using a collimated laser beam (He–Ne laser, 10 mW, λ = 532 nm) and a CCD camera containing 768 × 576 pixel array. Then, the pre-processing of speckle images is carried out to remove unwanted intensity variations due to ambient lighting change, etc. The spectral speckle correlation (auto-correlation) technique for surface roughness assessment have been used before and after pre-processing of speckle images then they are compared with the stylus values (R_a). It was found that autocorrelation parameters after pre-processing had a better correlation (i.e. higher correlation coefficient) with the average surface roughness (R_a) measured for the milled and ground components. This indicated the effectiveness of this approach of surface roughness evaluation using speckle correlation technique which is explained and analysed in this paper.

2. Laser speckle technique

2.1. Theory

The scattered light intensity of a rough surface is shown in Fig. 1. The lay and the roughness of the surface, which are characteristics of any machining process, determine the scattering pattern. A smooth surface scatters light mainly in a specular direction. It is reported that as the surface gets rougher, the specular component decreased and the scattering component was increasing. For a perfectly reflecting and an optically smooth surface with the heights of the surface irregularities much smaller than wavelength of the incident light, the relation between the scattered light and the surface roughness have been studied by use of vector diffraction and Bechmann scalar theory [16].

It is not easy to obtain an analytical value of the surface roughness from the light scattering pattern. Previous researchers Persson [17], Wang et al. [18] have shown that there is a good correlation existing between the scattered-light intensity distribution shown in Fig. 1 and surface roughness R_a. Density function $P(\varphi)$ of the scattered-light field from a rough surface

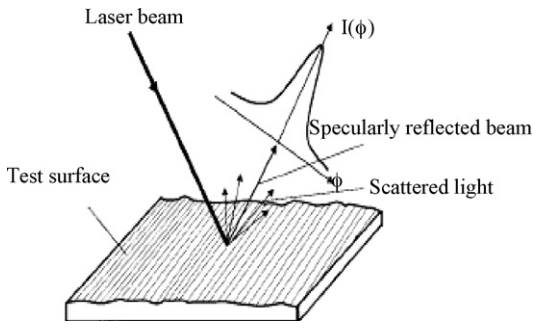

Fig. 1. Laser beam scattered from a rough surface and its corresponding light distribution.

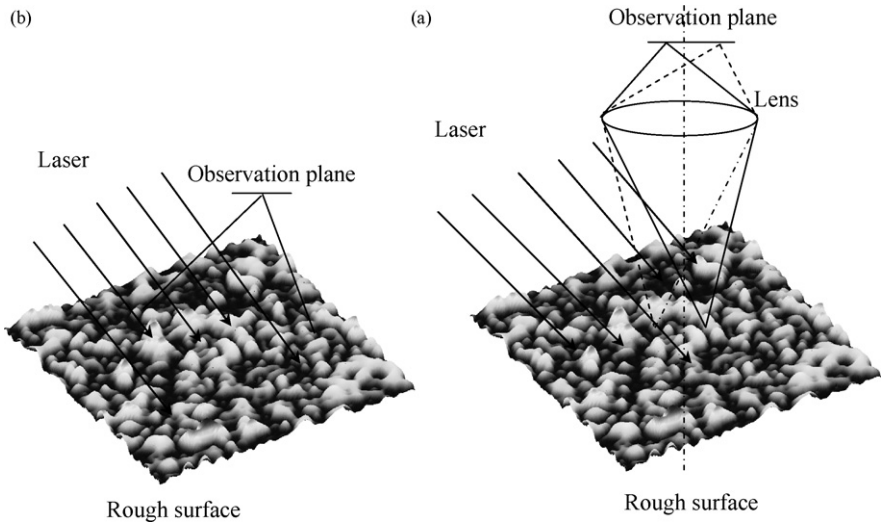

Fig. 2. Two basic schemes of speckle pattern formation.

can be normalized by light intensity $I(\varphi)$ as follows:

$$P(\varphi) = \frac{I(\varphi)}{\int_{-\pi/2}^{\pi/2} I(\varphi)\,\mathrm{d}\varphi} \quad (1)$$

The limits of integration from $-\pi/2$ to $\pi/2$ are the theoretical limits, but in practice the limits are determined by the aperture of the optical setup. The measurement procedures based on objective speckle phenomena are explained in the following discussion.

2.2. Properties

The basic configurations of the setup for surface roughness measurement by means of a speckle pattern are shown in Fig. 2. The speckle pattern formed in free space geometry is called objective speckles (Fig. 2a). Two substantial points should be generally mentioned for the objective speckle patterns. Basically, the contrast of the distribution depends mainly on the reflecting surface [19]. If the roughness of the surface (R_q) is less than $\lambda/4$ (a quarter of the illumination wavelength), the contrast increases proportional to the roughness up to unity. On the other hand, the average speckle size depends on the extension of illuminated spot on the object, as presented in Fig. 3. This speckle size can be easily calculated as $D_{obj} = k\lambda(L/d)$, where λ is the wavelength, d the diameter of the illuminated area, L the distance between the object and the screen and $k = 1.22$ which is the Rayleigh factor for pinhole apertures [20]. Alternatively, the speckle pattern that is formed by collecting the scattered light with a lens and focusing it onto a screen is called subjective speckle pattern, as shown in Fig. 2(b).

2.3. Evaluation of speckle scattering

The spatial properties of the speckle pattern can be related to the surface characteristics. For instance, surface roughness may be extracted from the information provided by speckle pattern. Over the past few decades since the invention of lasers, the relationship between surface roughness and speckle pattern has been widely investigated by many researchers. Models which describe the interaction between the statistical quantities of the speckle pattern and the statistical roughness parameters of the surface can be divided into static (speckle statistics) and dynamic methods (speckle correlation). Speckle statistics (speckle contrast) are based partly on the average light scattering properties and partly on the speckle-contrast relationship. The speckle correlation (auto-correlation function) is used mainly for smooth surfaces and it is bound up with the average speckle contrast, as well (the central value of an autocorrelation function is the standard deviation of the original signal).

3. Experimental setup

3.1. Specimens

The experiments were carried out by preparing flat specimens (mild steel) with different machining processes such as grinding and milling based on Box-Behnken approach [21]. Surfaces with different textures were obtained by controlling the machining parameters of these processes.

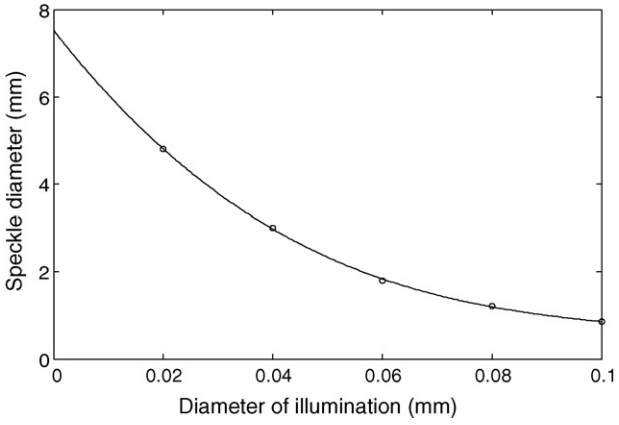

Fig. 3. Dependence of average speckle size on the diameter of illuminated area.

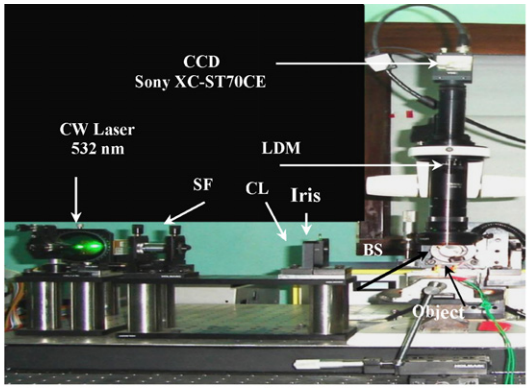

LDM=Long Distance Microscope; SF=Spatial Filter; VA=Variable Accumulator; CL=Collimating Lens; BS= Beam Splitter.

Fig. 4. Experimental setup for specklegram formation.

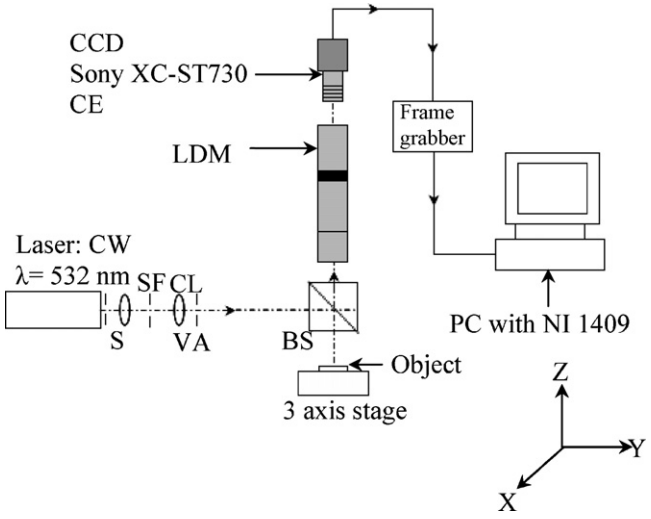

Fig. 5. Schematic diagram for experimental setup.

3.2. Experimental procedure

The experimental arrangement for recording of speckle images corresponding to different roughness of machined surfaces (ground and milled) is shown in Fig. 4. A schematic diagram explaining the experimental set up is shown in Fig. 5. Speckle pattern was formed by projecting the laser beam on to the specimen surface. A collimated laser beam (He–Ne laser, 10 mW, $\lambda = 532$ nm) is used to illuminate the object. To define and adjust the size of the laser beam, a beam expander and an aperture were used. The collimating lens (CL) was used to define the size of the illuminated spot. The size of the spot in these experiments was approximately 1 mm. The size of the speckles is affected by the size of the illuminated spot: the smaller the spot the larger will be the speckles. The size of the speckles must be adjusted so that each element in the detector is smaller than one speckle. The angle of registration and illumination is 90°. The emerging beam was focused using a microscope (4×). The real image formed was projected onto a CCD image sensor and displayed on a monitor simultaneously. The CCD camera is interfaced to a PC with a frame grabber card (NI1407). The speckle pattern was digitized by an image card with a 752×576 pixel array and using intensity resolution of 256 gray levels, from 0 (dark) to 255 (bright). The bright areas are the portions where constructive interference occurs and the dark spots are the results of destructive interference. The process of image acquisition with phase stepping is carried out with the support of Labview software. Only the central 300×300 pixels, representing an actual dimension of 2 mm × 2 mm, were chosen for analysis in order to prevent any edge effects. The odd (or even) number of rows of pixels were used only to eliminate the bewildering effect of interlace of the image, which is particularly important for tests on different machined surfaces. Monochromatic speckle patterns (Fig. 6) for ground and milled surfaces of $R_a = 1.842$ μm and $R_a = 2.509$ μm were recorded with a measuring arrangement shown in Fig. 4. The intensity distribution emerging from a smoother surface shows the speckle elongation phenomenon very clearly, which appears as a fibrous radial structure. In the case of the rougher surface, three independent monochromatic speckle patterns superimpose to an isotropic pattern with a pure stochastic intensity distribution. This effect is used for roughness characterization.

4. Pre-processing of surface images

A filter process had to be developed with which the unwanted intensity variations due to ambient lighting change and other

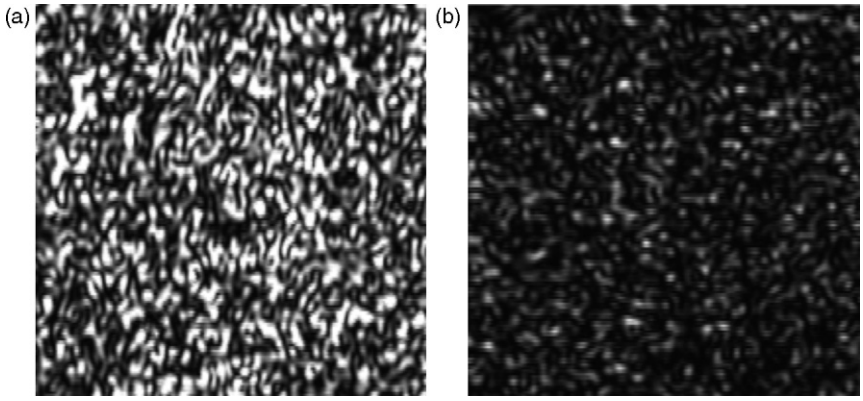

Fig. 6. CCD images (768×576 pixels) pf speckle patterns produced by: (a) ground surface of roughness $R_a = 1.842$ μm and (b) milled surface of roughness $R_a = 2.509$ μm.

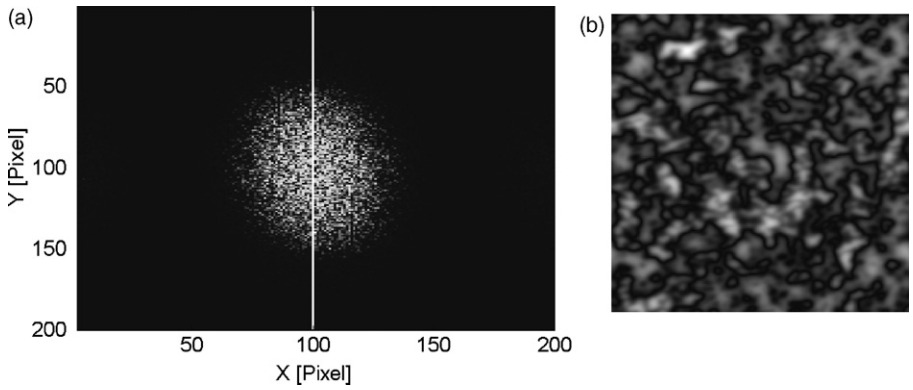

Fig. 7. Results of pre-processing of ground surface image (R_a = 1.842 μm): (a) amplitude density spectrum after FFT and (b) intensity distribution after inverse FFT.

effects not directly attributable to the roughness of the machined surfaces could be eliminated. Although the convolution filtering methods are faster and simpler, the exact separation of frequency ranges required the filtering in the spatial frequency domain. It needed further consideration that the Guass or exponential low-pass filter characteristics cut out also a part of the low-frequency spectrum that includes our measuring surface roughness. A cylinder filter can generate a hard oscillation in the back-transformed image because of its sharp cutting. That is because a Butterworth filter was realized with optimized characteristics whose steps are shown schematically in Figs. 7 and 8 for ground and milled surfaces. Figs. 7(a) and 8(a) are the centralized FFT function of the speckle pattern shown in Fig. 6(a) and (b). The frequency components resulting from the first scattering process are to seen as local rises on both sides of the one-dimensional low-frequency line in the middle. The functioning of the filter process is clearly noticeable in this figure. It cuts off the components that exceed a certain radius in the frequency domain (high frequency disturbance) as well as the one-dimensional line stretching through the spectrum (diffuse vertical intensity gradation in the original pattern). Figs.7(b) and 8(b) displays the intensity function transformed back after the filter process for ground and milled surfaces.

5. Surface roughness characterization using monochromatic speckle autocorrelation function

Correlation coefficients calculated by shifting two copies of the same measured speckle pattern against each other compose the discrete auto-correlation function. The central gradient, i.e. the fall speed of this function is considered to be the roughness parameter. It is more expedient to use the normalized autocorrelation function (ACF), given by

$$\mathrm{AC} = \frac{\sum_{i=1}^{M}\sum_{j=1}^{N}(g(i,\,j)-\bar{g})(g(i+\delta i,\,j+\delta j)-\bar{g})}{\sum_{i=1}^{M}\sum_{J=1}^{N}(g(i,\,j))^2} \tag{2}$$

where $g(i,j)$ is the intensity function of the speckle structure, $\delta i = 1, \ldots, M$, $\delta j = 1, \ldots, N$ are the pixel shift values and $\bar{g}$ is the mean intensity. The normalized cut section of two-dimensional autocorrelation function for ground and milled surfaces are shown in Fig. 9. Several auto-correlation parameters after filtering are tested to examine the relationship between the digitized speckle pattern and surface roughness.

The parameters used in this study are the following:

(a) Integrated autocorrelation coefficient IACX

IACX is determined by shifting the image in the x-direction with a lag length δj that varies between 1 and N.

$$\mathrm{IACX} = \sum_{i=1}^{M}\frac{\sum_{i=1}^{M}\sum_{j=1}^{N-\delta j} g(i,\,j)\mathrm{X}\, g(i,\,j+\delta j)}{\sum_{i=1}^{M}\sum_{j=1}^{N} g^2(x,\,y)} \tag{3}$$

(c) Integrated autocorrelation coefficient IACY.

IACY is calculated by shifting the image in the y-direction with a lag length δi that varies between 1 and M

$$\mathrm{IACY} = \sum_{i=1}^{M}\frac{\sum_{i=1}^{M-\delta i}\sum_{j=1}^{N} g(i,\,j)\mathrm{X}\, g(i,\,j+\delta j)}{\sum_{i=1}^{M}\sum_{j=1}^{N} g^2(x,\,y)} \tag{4}$$

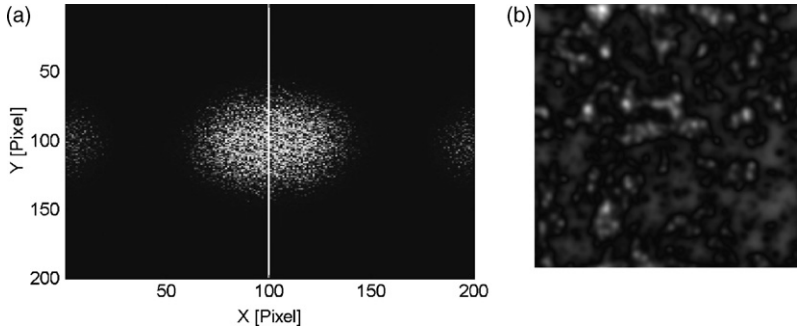

Fig. 8. Results of pre-processing of milled surface image (R_a = 2.509 μm): (a) amplitude density spectrum after FFT and (b) intensity distribution after inverse FFT.

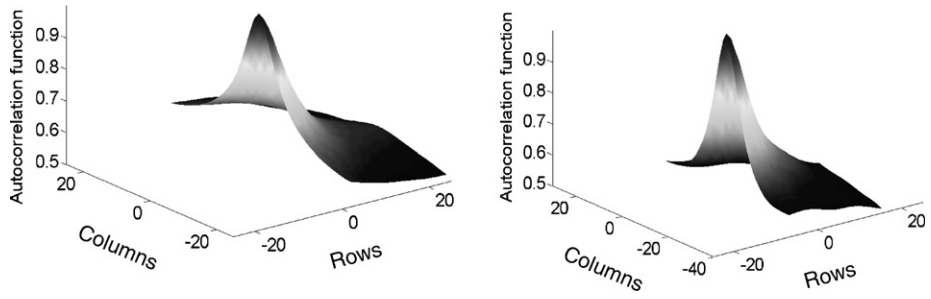

Fig. 9. Cut section of two-dimensional ACF's of 256 × 256 pixel arrays of the speckle patterns according to Figs. 7(b) and 8(b).

(d) Integrated autocorrelation coefficient IACXY.

IACXY is calculated by shifting in the diagonal direction

$$\mathrm{IACXY} = \sum_{i=1}^{M} \frac{\sum_{i=1}^{M-\delta i}\sum_{j=1}^{N-\delta j} g(i,\, j)\mathrm{X}\, g(i+\delta i,\, j+\delta j)}{\sum_{i=1}^{M}\sum_{j=1}^{N} g^2(x,\, y)} \tag{5}$$

For Eqs. (3)–(5), autocorrelation involves shifting the image by a lag length δ and the shifted object is used as virtual image for correlation analysis with the original one. The shift may be done in the x,y or diagonal direction.

(e) Average peak spectral intensity coefficient, HA.

HA is defined as the ratio between the average peak spectral value and the average peak spectral value at smoothest surface.

$$\mathrm{HA} = \frac{1/M\sum_{k=1}^{M} g(ik,\, jk)}{1/N\sum_{k=1}^{M} g_0(ik,\, jk)} \tag{6}$$

(f) Integrated peak spectral intensity coefficient, HI.

HI is defined as the ratio between the sum of peak spectral values and the sum of peak spectral values at smoothest surface.

$$\mathrm{HI} = \frac{\sum_{k=1}^{M} g(ik,\, jk)}{\sum_{k=1}^{M} g_0(ik,\, jk)} \tag{7}$$

The above autocorrelation parameters after pre-processing of speckle images are calculated for surfaces produced by different machining processes (grinding and milling) and are shown in Tables 1 and 2 for the assessment of surface roughness. The stylus surface roughness parameter chosen for comparison is the average surface roughness (R_a) as it is the most widely used and accepted by researchers and in industry as well [22].

6. Results and discussions

The surface roughness is characterized by the widths of 2D-autocorrelation functions, which can be obtained from digital processing of these images As it is shown in autocorrelation diagram (Fig. 9) after pre-processing, the form of the ACF's changes with the roughness. Since the autocorrelation functions are normalized, their values are unity in the origin. By increasing the shift the autocorrelation values fall in all cases and the curves converge to a constant value depending on the roughness as plotted in Fig. 10 (the trajectories are drawn mirrored and the arrow shows the direction of increasing roughness). A faster of data capture and evaluation can be realized by the use of a CCD line sensor. The measuring effect based on this technique is illustrated in Figs. 11 and 12. In Fig. 11, the gray-level data of arbitrarily chosen line 50 of the CCD images according to Figs.7(b) and 8(b) are depicted. These plots show that an increasing surface roughness leads to an increase of the speckle-intensity fluctuations. It also seen from Fig. 11 that the smooth ground surfaces, reflected more light than the rough milled surfaces. Hence, the speckle image of ground specimen contained elements with high gray values. This can be obtained quantitatively by the width of the corresponding ACF, as shown in Fig. 12.

Figs. 13 and 14 shows the variation of IACX, IACY and IACXY with surface roughness before and after pre-processing

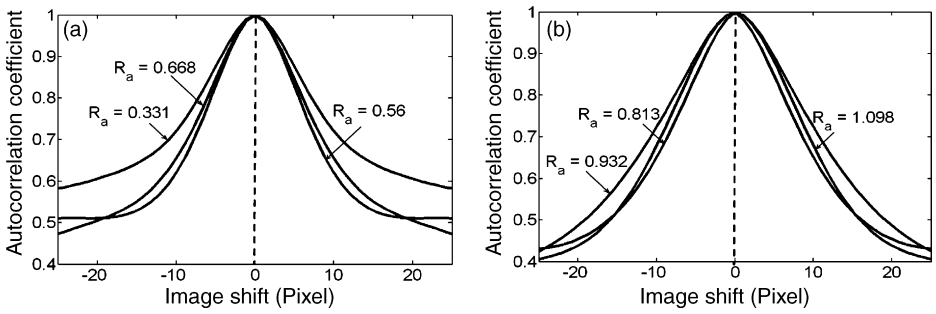

Fig. 10. The calculated trajectories of autocorrelation of speckle pattern images: (a) ground surfaces and (b) milled surfaces after pre-processing.

Table 1
Machining and auto correlation parameters used (ground) and the corresponding roughness values of the components

S. no	Machining condition			Before pre-processing					After pre-processing					Stylus values
	Speed (rpm)	Feed (mm/min)	Depth of cut (mm)	Integrated autocorrelation coefficient			Integrated spectral intensity		Integrated autocorrelation coefficient			Integrated spectral intensity		R_a (μm)
				IACX	IACY	ICAXY	HA	HI	IACX	IACY	ICAXY	HA	HI	
1	1500	13	0.4	142.18	139.5	139.1	1.33	1.93	149.5	148.5	147	1.197	1.367	1.891
2	1900	13	0.4	141.18	137.8	139.2	1.24	1.93	149.5	148.8	147	1.183	1.36	1.842
3	1500	17	0.4	135.86	133.4	132.1	0.92	1.72	144.7	142.7	141	1.134	1.24	1.153
4	1900	17	0.4	137.95	134.9	134.6	1.19	1.87	147.2	146.3	144.6	1.163	1.31	1.618
5	1500	15	0.2	138.93	137.4	135.7	1.24	1.92	148	148.2	147.8	1.177	1.36	1.831
6	1900	15	0.2	138.16	135	134.7	1.19	1.89	148.8	145.7	143.8	1.169	1.32	1.691
7	1500	15	0.6	128.89	126.3	126.8	0.67	1.12	133.6	130.4	129.7	0.951	1.05	0.341
8	1900	15	0.6	138.82	135.1	135.6	1.23	1.89	147.9	146.3	144.8	1.171	1.33	1.694
9	1700	13	0.2	137.54	134.6	133.6	1	1.85	146.5	144.3	142.9	1.163	1.297	1.483
10	1700	17	0.2	130.17	128.2	127.1	0.72	1.3	138	131.3	132.7	1.017	1.087	0.393
11	1700	13	0.6	135.29	131.4	131	0.75	1.56	141.9	137.6	136.4	1.077	1.143	0.668
12	1700	17	0.6	132.02	128.7	129.8	0.74	1.32	139.6	136.7	135.4	1.043	1.11	0.56
13	1700	15	0.4	132.36	131.3	130.4	0.74	1.55	140.3	137	136.3	1.05	1.126	0.614
14	1700	15	0.4	130.12	128.7	127	0.71	1.24	137.5	130.5	130	0.983	1.08	0.383
15	1700	15	0.4	128.45	125.2	124.1	0.55	1	134	129	127.9	0.951	1	0.331

IACX = integrated autocorrelation coefficient in X-direction; IACY = integrated autocorrelation coefficient in Y-direction; IACXY = integrated autocorrelation coefficient in XY-direction; HA = average peak spectral intensity coefficient; HI = integrated peak spectral intensity coefficient.

Table 2
Machining and auto correlation parameters used (milled) and the corresponding roughness values of the components

S. no	Machining condition			Before pre-processing					After pre-processing					Stylus values
	Speed (rpm)	Feed (mm/min)	Depth of cut (mm)	Integrated autocorrelation coefficient			Integrated spectral intensity		Integrated autocorrelation coefficient			Integrated spectral intensity		R_a (μm)
				IACX	IACY	ICAXY	HA	HI	IACX	IACY	ICAXY	HA	HI	
1	800	50	0.3	135.29	132.0	132.0	1.4	1.09	133.3	125.2	123.31	1.17	1.64	1.291
2	1200	50	0.3	136.35	133.1	132.5	1.5	1.18	133.1	126.1	121	1.20	1.68	1.307
3	800	150	0.3	127.45	122.6	120.6	1.1	1	123	104.7	103.82	1.00	1	0.813
4	1200	150	0.3	136.84	134.1	135.2	1.6	1.24	131.3	126.2	123.5	1.30	1.70	1.393
5	800	100	0.2	131.22	126.6	121.9	1.3	1.01	125.5	114.2	111.2	1.00	1.29	1.081
6	1200	100	0.2	130.70	125.9	120.8	1.3	1.0	126.1	111	107.65	1.00	1.23	0.932
7	800	100	0.4	142.99	141.4	139.8	1.8	1.42	136.7	133.1	138.4	1.39	1.86	1.788
8	1200	100	0.4	135.16	131.2	131.9	1.4	1.05	128.3	120.6	122.55	1.03	1.52	1.098
9	1000	50	0.2	141.85	138.4	136.5	1.7	1.31	133.9	128.3	125.8	1.34	1.76	1.459
10	1000	150	0.2	144.21	144.0	145.1	1.9	1.47	142	142.6	147.1	1.53	2.09	2.457
11	1000	50	0.4	154.19	153.8	150.7	2.0	1.54	143.7	146.8	149.76	1.63	2.18	2.653
12	1000	150	0.4	133.71	127.8	128.9	1.3	1.02	133	116.2	111.3	1.01	1.38	1.083
13	1000	100	0.3	142.23	138.5	138.1	1.8	1.35	134.4	130	129.7	1.35	1.78	1.522
14	1000	100	0.3	146.16	144.3	146.6	1.9	1.49	142.1	141.7	142.36	1.57	2.1	2.509
15	1000	100	0.3	141.01	138.3	136.1	1.7	1.31	133.6	130.3	128.76	1.33	1.75	1.433

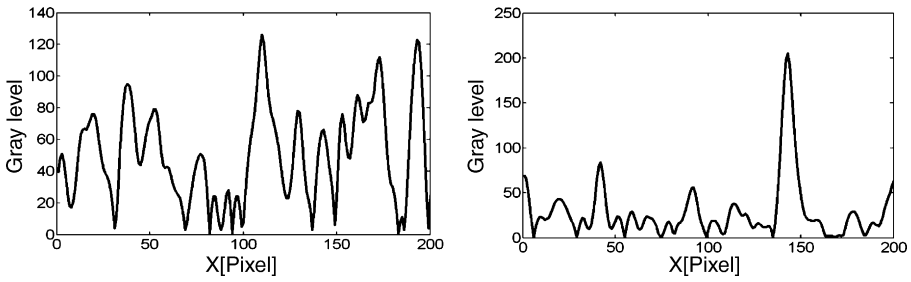

Fig. 11. Gray-level data of CCD line number 50 of the speckle pattern images shown in Figs. 7(b) and 8(b), respectively.

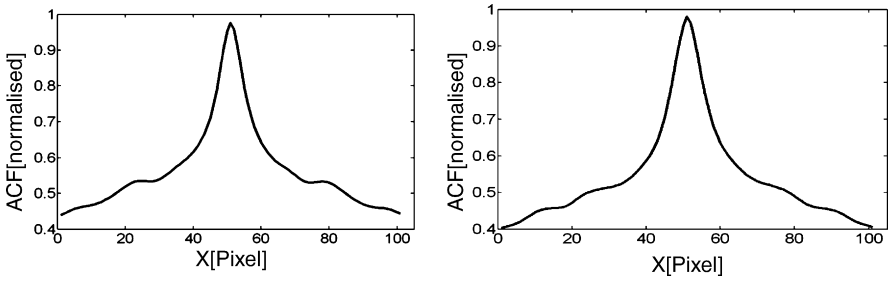

Fig. 12. One-dimensional ACF's of 512 pixels of the CCD line according to Figs.7(b) and 8(b) in the vicinity of the origin located at pixel position 50.

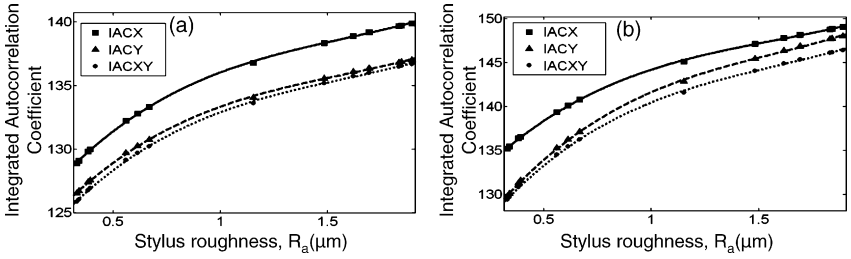

Fig. 13. Correlation of estimated roughness values and integrated autocorrelation coefficient: (a) before pre-processing and (b) after pre-processing for ground surface.

for ground and milled surfaces. Positive correlation is observed for the entire surface-roughness. The relationship are fitted using the empirical equations as shown below.

6.1. Before pre-processing of surface image

Grinding

$$\text{IACX} = 6.3091 \ \ln(R_a) + 135.88, \qquad R^2 = 0.9445$$

$$\text{IACY} = 6.0152 \ \ln(R_a) + 133.19, \qquad R^2 = 0.9257$$

$$\text{IACXY} = 6.2172 \ \ln(R_a) + 132.75, \qquad R^2 = 0.9099$$

Milling

$$\text{IACX} = 18.304 \ \ln(R_a) + 132.09, \qquad R^2 = 0.8873$$

$$\text{IACY} = 22.432 \ \ln(R_a) + 127.48, \qquad R^2 = 0.9198$$

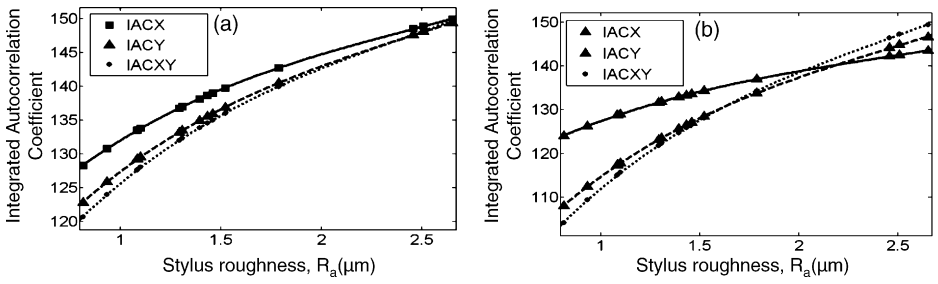

Fig. 14. Correlation of estimated roughness values and integrated autocorrelation coefficient: (a) before pre-processing and (b) after pre-processing for milled surface.

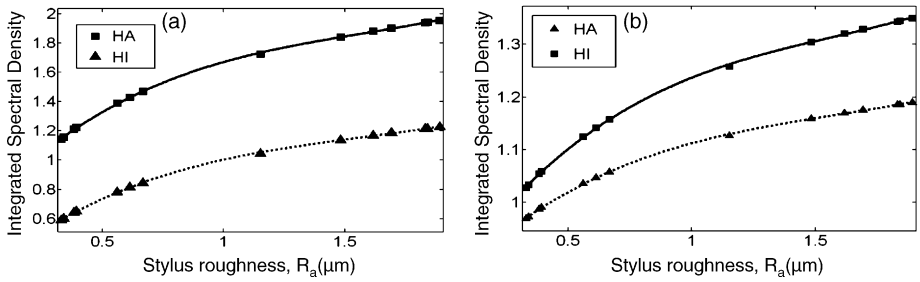

Fig. 15. Correlation of estimated roughness values and spectral intensity: (a) before pre-processing (b) after pre-processing for ground surface.

$$\text{IACXY} = 24.484\ \ln(R_a) + 125.74, \qquad R^2 = 0.9293$$

6.2. After pre-processing of surface image

Grinding

$$\text{IACX} = 7.9483\ \ln(R_a) + 143.99, \qquad R^2 = 0.9726$$

$$\text{IACY} = 10.469\ \ln(R_a) + 141.35, \qquad R^2 = 0.9883$$

$$\text{IACXY} = 9.7808\ \ln(R_a) + 140.21, \qquad R^2 = 0.9114$$

Milling

$$\text{IACX} = 16.452\ \ln(R_a) + 127.45, \qquad R^2 = 0.9284$$

$$\text{IACY} = 32.667\ \ln(R_a) + 114.8, \qquad R^2 = 0.9627$$

$$\text{IACXY} = 38.29\ \ln(x) + 112.06, \qquad R^2 = 0.9499$$

Figs. 15 and 16 illustrate the variation of HA and HI with surface-roughness. The values of HI are higher than HA for each surface-roughness. These relationships may also be fitted using the following empirical equations.

6.3. Before pre-processing of surface image

Grinding

$$\text{HA} = 0.3655\ \ln(R_a) + 0.9936, \qquad R^2 = 0.9267$$

$$\text{HI} = 0.4656\ \ln(R_a) + 1.6583, \qquad R^2 = 0.9614$$

Milling

$$\text{HA} = 0.7627\ \ln(R_a) + 1.3625, \qquad R^2 = 0.9195$$

$$\text{HI} = 0.5213\ \ln(R_a) + 1.0513, \qquad R^2 = 0.9256$$

6.4. After pre-processing of surface image

Grinding

$$\text{HA} = 0.1266\ \ln(R_a) + 1.109, \qquad R^2 = 0.979$$

$$\text{HI} = 0.1847\ \ln(R_a) + 1.232, \qquad R^2 = 0.981$$

Milling

$$\text{HA} = 0.5945\ \ln(R_a) + 1.0482, \qquad R^2 = 0.9312$$

$$\text{HI} = 0.9087\ \ln(R_a) + 1.3406, \qquad R^2 = 0.9379$$

It can be observed that the IACX, IACY and IACXY, HA and HI values follow similar trends with surface-roughness. All these parameters increase logarithmically with surface-roughness with IACY showing excellent correlation for both ground ($R^2 = 0.9883$) and milled ($R^2 = 0.9627$) surfaces after pre-processing the images. This indicates clearly that IACY would be a more suitable parameter for surface-roughness measurement. To determine the repeatability of the proposed measurement technique roughness measurements were made at different places on a component number of times. Tables 3 and 4 show the vision roughness parameter values (IACY) after pre-processing and stylus roughness values obtained for a ground and milled specimens for six trials. The variability of the proposed method is less, showing consistent results. The repeatability of the proposed technique for both ground (CV = 1.357) and milled (CV = 2.191) is good. This could be due to the fact [23] that the proposed method is based on area sampling while stylus instruments does line sampling.

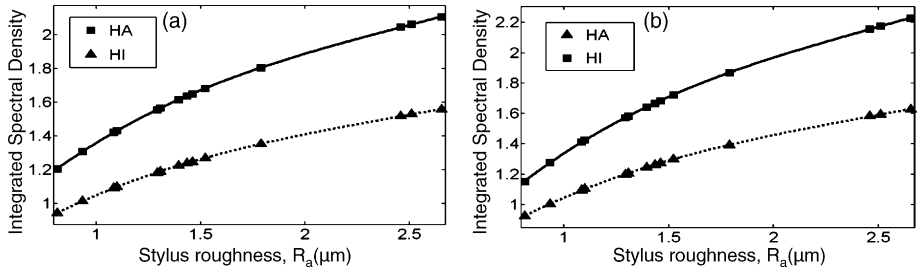

Fig. 16. Correlation of estimated roughness values and spectral intensity: (a) before pre-processing and (b) after pre-processing for milled surface.

Table 3
Precision of the roughness measurement for ground surfaces by the proposed technique

S. no	Stylus roughness, R_a (μm)	Vision roughness, R_v (μm)
1	3.01	2.79
2	2.032	1.94
3	1.132	0.577
4	0.986	0.515
5	0.863	0.421
6	2.012	1.589
Average	1.672	1.306
S.D.	0.831	0.964
CV	2.012	1.357

Note: CV = coefficient of variation; S.D. = standard deviation.

Table 4
Precision of the roughness measurement for milled surfaces by the proposed technique

S. no	Stylus roughness (R_a) (μm)	Vision roughness (R_v) (μm)
1	1.23	1.194
2	2.5	2.801
3	2.865	3.351
4	2.854	3.465
5	2.012	1.693
6	1.426	1.228
Average	2.148	2.289
S.D.	0.710	1.044
CV	3.026	2.191

Note: CV = coefficient of variation; S.D. = standard deviation.

7. Conclusions

An experimental investigation has been performed to study the improved implementation of the laser speckle technique as a sensitive non-contact tool for measuring surface roughness. Pre-processing of images of speckle pattern has been carried out to improve the quantification of roughness parameters.

The results of estimation of surface roughness of ground and milled surfaces based on the speckle patterns obtained before and after pre-processing were compared. There was a clear indication of improvement in correlation of results after pre-processing the speckle patterns.

The correlation of estimated surface roughness values based on speckle patterns with stylus R_a values indicate clearly the possibility of successful implementation of the presented approach in practice.

Acknowledgment

This research is supported by Defense Research Development Organization (DRDO), India.

References

[1] Whitehouse DJ. Stylus contact method for surface metrology in the ascendancy. Meas Cont 1998;31(2):48–50.
[2] Whitehouse DJ. Handbook of Surface and Nanometrology. London: Institute of Physics Publishing (IOP); 2003.
[3] Lenz FY, Shamir J. Optical profiler. A new method for high sensitivity and wide dynamic range. J Appl Opt 1982;21:3200–8.
[4] O'Donell KA. Effects of finite stylus width in surface contact profilometry. J Appl Opt 1993;25:4922–8.
[5] Kiran M, Ramamoorthy B, Radhakrishnan V. Evaluation of surface roughness by vision system. Int J Machine Tools Manuf 1998;38:685–90.
[6] Persson U. Real time measurement of surface roughness on ground surfaces using speckle-contrast technique. Opt Laser Eng 1992;17:61–7.
[7] Persson U. Measurement of surface roughness on rough machined surface using speckle correlation and image analysis. Wear 1993;160:221–5.
[8] Ruffung B. Application of speckle-correlation methods to surface roughness measurement: a theoretical study. J Opt Soc Am 1986;A3:1297–304.
[9] Tay CJ, Toh SL, Shang HM, Zhang JB. Whole field determination of surface roughness by speckle correlation. J Appl Opt 1995;34:2324–35.
[10] Beckmann P. The scattering of light by rough surfaces. Prog Opt 1967;6:53–68.
[11] Fujii H, Asakura T, Shindo Y. Measurement of surface roughness properties by using image speckle contrast. J Opt Soc Am 1976;66:1217–21.
[12] Sprague RA, Thompson BJ. Quantitative visualization of large variation phase objects. J Appl Opt 1972;11:1469–79.
[13] Yoshimura T, Kato K, Nakagawa K. Surface roughness dependence of the intensity correlation function under speckle pattern illumination. J Opt Soc Am 1990;7:2254.
[14] Yamaguchi I, Kobayashi K, Yaroslavsky L. Measurement of surface roughness by speckle correlation. Soc Photo-Optical Instrum Eng 2004;43(11):2753–61.
[15] Lukaszewsk K, Rozniakowski K, Wojtatowicz T. Laser examination of cast surface roughness. Soc Photo-Optical Instrum Eng 2001;40(9):1993–7.
[16] Elson JM, Bennett JM. Vector scattering theory. J Opt Eng 1979;18:116–24.
[17] Persson U. Measurement of surface roughness using infrared scattering. Measurement 1996;18:109–16.
[18] Wang SH, Quan C, Tay CJ, Shang HM. Surface roughness measurement in the submicrometer range using later scattering 2000;39:1591–1601.
[19] Dainty JC. Laser Speckle and Related Phenomena. New York: Springer; 1984.
[20] Sirohi RS. Speckle Metrology. New York: McGraw-Hill; 1998.
[21] Box GEP, Behnken DW. Technometrics 1960;2:455.
[22] ISO 4288:1996, Geometrical product specification (GPS)-surface texture: profile method-terms definitions and surface texture parameters, Inst. Std. Org., Geneva.
[23] Luk F, Huynh V, North W. Measurement of surface roughness by a machine vision. J Phys E Sci Instrum 1989;22:977–80.